Structural features of new rare earth-based mixed anions (O, S, F) compounds: relationships between optical absorption and rare earth environment

Damien Pauwels, Alain Demourgues, Hervé Laronze, Pierre Gravereau, François Guillen, Olivier Isnard, Alain Tressaud

Structural features of new rare earth-based mixed anions (O, S, F) compounds: relationships between optical absorption and rare earth environment

Damien Pauwels [a,*], Alain Demourgues [a,b], Hervé Laronze [a], Pierre Gravereau [a], François Guillen [a], Olivier Isnard [c], Alain Tressaud [a]

[a] *ICMCB-CNRS, 87 avenue du Dr A. Schweitzer, 33608 Pessac Cedex, France*
[b] *RHODIA, CRA, 52 rue de la Haie Coq, 93308 Aubervilliers Cedex, France*
[c] *Laboratoire de cristallographie, avenue des martyrs, 38042 Grenoble Cedex, France*

Abstract

In the structure of α-LnSF and $Ln_2AF_4S_2$ (A = Ca, Sr) compounds which can be considered as formed of layer stacking, the rare earth and fluorine atoms form $[Ln_2F_2]^{4+}$ or $[Ln_2AF_4]^{4+}$ fluorite-type blocks which alternate with double $[S_2]^{4-}$ layers along the *c*-axis. Then, it appears possible to modify the size of the fluorite-type block without any modification of its charge. In the case of rare earth oxyfluorosulfides, two new classes of compounds $Ln_3OF_3S_2$ (Ln = La, Ce) and $La_2O_{1.5}FS$ were identified. The structures of these compounds are related to α-LnSF and Ln_2O_2S networks. In these frameworks, the charge of the blocks containing the rare earth ions can be 2+ or 4+. These blocks alternate with single or double layers of sulfur atoms. The local geometry (number of neighbors, bond distances and angles) around the rare earth varies as a function of the number of the sulfur sheets. Absorption properties in UV-visible range are correlated with the structural features.

Keywords Rare earth; Fluorosulfides; Oxyfluorosulfides; Powder X-ray/neutron diffraction; Structure refinement; UV-visible absorption; Electronic transitions

1. Introduction

The rare earth-based mixed anions compounds containing sulfur atoms have been largely investigated for their specific properties in absorption and luminescence fields. The rare earth oxysulfides Ln_2O_2S are mainly used as luminescent materials. The red-emitting Y_2O_2S: Eu^{3+} is a cathode-ray phosphor present in color TV screens [1]. For the conventional intensifying screens used in radiography, one of the best X-ray phosphors is the Gd_2O_2S: Tb^{3+} compound, which emits in the green [2]. The rare earth fluorosulfides LnSF are good candidates as new inorganic color pigments [3]. They exhibit good chromatic properties and high stability in acidic medium.

The presence in the vicinity of rare earth ions ($4f$ and $5d$ shells) of more than two anions (p shell) with various polarizabilities leads to an alteration of the energetic parameters such as the bandwidth and the position of p and $5d$ bands, as well as those of $4f$ levels, thus giving these unique optical properties.

Because of their various sizes and charges, anions can occupy various crystallographic sites. For instance, the Ln_2O_2S and LnSF structures exhibit a stacking of layers due to the occurrence of sulfur and oxygen/fluorine atoms in two different sites. The Ln_2O_2S compounds have a hexagonal symmetry, closely related to the La_2O_3 type. In this structure the $[Ln_2O_2]^{2+}$ sheets and single sulfur atoms layers are stacked along the c direction. The LnSF compounds crystallize with the PbFCl type structure. Numerous compounds adopt a structure deriving from the PbFCl type which can be described as a succession of $[Pb_2F_2]^{2+}$ sheets and $[Cl_2]^{2-}$ layers. In order to study the correlations between

* Corresponding author.
E-mail address pauwels@icmcb.u-bordeaux.fr (D. Pauwels).

structural features and UV-visible absorption, the synthesis of rare earth oxysulfides (Ln_2O_2S), fluorosulfides (LnSF, $Ln_2CaF_4S_2$) as reference compounds has been firstly undertaken. A new series of mixed anions compounds containing rare earth, $Ln_3OF_3S_2$ (Ln = La, Ce) and $La_2O_{1.5}FS$ have been prepared by solid state routes. The structures have been respectively determined and refined on the basis of single crystal and powder X-ray diffraction analysis, and powder neutron diffraction data in the case of the $La_2O_{1.5}FS$ phase. The diffuse reflectance spectra have been recorded for the lanthanum-based compounds and the optical absorption of these samples has been discussed in term of crystal field and nephelauxetic effects related to the rare earth environment.

2. Experimental

2.1. Preparation of materials

Rare earth α-LnSF, $Ln_2CaF_4S_2$ fluorosulfides, Ln_2O_2S oxysulfides, $Ln_3OF_3S_2$ and $Ln_2O_{1.5}FS$ oxyfluorosulfides were synthesized by reaction of stoichiometric quantities of high purity rare earth sulfides in their α form, rare earth fluorides, calcium fluoride and rare earth oxides. Fluorides were purified under F_2 or HF at temperatures varying from 500 to 800 °C. α-Ln_2S_3 sulfides were prepared starting from reaction involving pure rare earth metal and sulfur slowly heated in sealed quartz tubes at 400 °C for 24 h, then 700 °C for 24 h. These starting materials were mixed under a dry argon atmosphere in a glove box because of their sensitivity to oxygen and moisture. For α-LnSF and Ln_2O_2S (Ln = La–Gd), the reactions were carried out in a platinum crucible placed in a quartz tube which was sealed under vacuum and heated up to 900 °C for 24 h. In the case of $Ln_2CaF_4S_2$ (Ln = La–Gd), $La_2O_{1.5}FS$ and $Ln_3OF_3S_2$ (Ln = La, Ce), the mixture was heated up to 1100 °C. In order to obtain single crystals of $Ln_3OF_3S_2$, the mixture was slowly heated up to 1200 °C (15 °C/h) and slowly cooled down to room temperature (5 °C/h).

The amount of fluorine and sulfur in the compounds was determined by chemical analysis. In the case of fluorine, the samples were dissolved in a flux of $CaCO_3/KCO_3$ at 840 °C and the amount of the fluorine measured by a LaF_3 specific electrode. For the sulfur determination, the samples were heated at 1300 °C with formation of SO_2. The quantity of SO_2 was measured by means of infrared spectroscopy. Particles size and distribution of these five compounds are quite identical, i.e. around 10 μm.

2.2. X-ray and neutrons diffraction experiments. Diffuse reflectance spectroscopy

Weissenberg and precession photographs of $Ce_3OF_3S_2$ single crystal showed an orthorhombic symmetry belonging to the Laue class *mmm* with systematic extinctions ($h0l$: $h + l = 2n + 1$ and $0kl$: $k + l = 2n + 1$) consistent with space group *Pnnm*. Intensity data were collected on an Enaf Nonius CAD4 four circle diffractometer using graphite monochromated Mo Kα radiation over the half reciprocal space group. Intensity treatment and refinement calculations were performed using the JANA 2000 program [4]. The quality of the acquisition and refinement was based on the conventional reliability factors R_{int} and R, wR, respectively.

Powder X-ray diffraction profiles of $La_3OF_3S_2$ and $La_2O_{1.5}FS$ were recorded on a Philips PW 1050 diffractometer in a Bragg–Bentano geometry, using monochromated Cu $K\alpha$ radiation. Data were collected over $5° \leqslant 2\theta \leqslant 120°$ with 0.02° steps and integration time of 40 s. The neutron diffraction patterns of $La_2O_{1.5}FS$ were obtained on the D1B diffractometer of the Institut Laue Langevin (ILL) at Grenoble, France ($\lambda = 1.28$ Å; 0.2° step scan; 8.0°–87.25° (2θ) angular range).

$La_2O_{1.5}FS$ crystallizes with hexagonal symmetry in P-3m1 space group whereas the $La_3OF_3S_2$ unit cell is orthorhombic and adopts *Pnnm* space group. The structure refinements of both phases were carried out using the Rietveld method. The RIETICA 1.72 program package [5] was used. R_p and R_{wp} reliability factors discussed in this paper were the usual ones defined by the Rietveld method.

The XRD patterns of prepared LnSF, Ln_2O_2S and $Ln_2CaF_4S_2$ and the refinement of the unit cell parameters are in good agreement with the reported data [3,6,7].

Diffuse reflectance spectra were recorded on a Cary 17 spectrophotometer in the UV-visible region.

3. Results

3.1. Structure determination

The structural parameters of α-LnSF, $Ln_2CaF_4S_2$ and La_2O_2S compounds have been previously determined [3,7].

3.1.1. $Ln_3OF_3S_2$ (Ln = La, Ce)

A microprobe analysis on Ce-based single crystals confirms the $Ce_3OF_3S_2$ formula. The structure of $Ce_3OF_3S_2$ has been solved in the *Pnnm* space group (n° 58) in agreement with the Weissenberg and precession photographs. Atoms have been placed by considering conventional Patterson methods associated with a difference Fourier synthesis. The final reliability factor $R_{\text{int}} = 2.89\%$, $R = 3.33\%$ and $wR = 2.73\%$ associated to 1809 reflections considering isotropic atomic displacement are rather small (Table 1). Anisotropic atom displacement does not improve the refinement result. The atomic position of the heavy element Ce has been firstly determined and corresponds to 8h (x, y, z) and 4g $(x, y, 0)$ positions. Another 8h site is fully occupied by S atoms and two 4e $(0, 0, z)$ sites are occupied by fluorine atoms. On the other hand two 8h sites are half occupied by fluorine and oxygen atoms. It can be noted that the 4f positions (0, ½, z), close to the previous 8h ones, could not be taken into account because the isotropic thermal

Table 1
Atomic positions, isotropic thermal displacement and reliability factor of $Ce_3OF_3S_2$ (single crystal analysis) and $La_3OF_3S_2$, $La_2O_{1.5}FS$ (powder Rietveld analysis)

$Ce_3OF_3S_2$ (*Pnnm*), X-ray refinement (single crystal)
$a = 5.743(2)$ Å, $b = 5.725(2)$ Å, $c = 19.391(4)$ Å, $R_{int} = 2.89\%$, $R = 3.33\%$, $wR = 2.73\%$

Atoms	Site	x	y	Z	U_{iso} (Å^2)	Occupancies
Ce1	4g	0.2592(4)	0.2628(2)	0	0.0125(2)	1
Ce2	8h	0.7487(4)	0.2621(1)	0.15538(2)	0.0113(1)	1
S	8h	0.748(1)	0.2612(4)	0.3058(1)	0.0104(4)	1
F1	4e	0	0	0.430(1)	0.0027(19)	1
F2	8h	0.564(2)	0.061(3)	0.059(1)	0.019(3)	0.5
F3	4e	0	0	0.073(2)	0.017(2)	1
O	8h	0.455(3)	0.048(3)	0.431(1)	0.011(3)	0.5

$La_3OF_3S_2$ (*Pnnm*), X-ray refinement, $R_p = 15.96\%$, $R_{wp} = 7.71\%$
$a = 5.804(2)$ Å, $b = 5.784(2)$ Å, $c = 19.482(5)$ Å

Atoms	Site	x	y	Z	U_{iso} (Å^2)	Occupancies
La1	4g	0.2597(4)	0.256(2)	0	0.0117(5)	1
La2	8h	0.7488(2)	0.258(3)	0.155(1)	0.0114(2)	1
S	8h	0.744(4)	0.257(6)	0.304(3)	0.0112(6)	1
F1	4e	0	0	0.427(2)	0.008	1
F2	8h	0.56(2)	0.053(2)	0.061(2)	0.008	0.5
F3	4e	0	0	0.076(2)	0.008	1
O	8h	0.45(3)	0.047(3)	0.430(2)	0.008	0.5

$La_2O_{1.5}FS$ (P-3m1), Neutron refinement, $R_p = 2.05\%$, $R_{wp} = 2.76\%$
$a = 4.111(7)$ Å, $c = 6.917(9)$ Å, X-ray refinement, $R_p = 10.42\%$, $R_{wp} = 6.05\%$

Atoms	Site	x	y	Z	B_{eq} (Å^2)	Occupancies
La	2d	2/3	1/3	0.2801(2)	0.87(5)	1
S	1a	0	0	0	0.192(9)	1
F/O1	2d	2/3	1/3	0.6342(3)	1.236(8)	1
F/O2	6i	0.0743(5)	−0.0749	0.4552(3)	3.1(1)	0.0833

Table 2
Interatomic distances in $Ce_3OF_3S_2$

$Ce_3OF_3S_2$ interatomic distances			
Ce1–F1	2.370(14) × 2	Ce2–S	2.968(7) × 1
Ce1–F2	2.398(19) × 2	Ce2–S	2.954(2) × 1
Ce1–F3	2.550(16) × 2	Ce2–F1	2.567(15) × 2
Ce1–O	2.44(2) × 2	Ce2–F2	2.42(2) × 2
Ce2–S	2.919(2) × 1	Ce2–F3	2.623(18) × 2
Ce2–S	2.975(7) × 1	Ce2–O	2.33(2) × 2
Ce2–S	2.965(2) × 1		

displacement was too high for these sites ($U_{iso} \approx 0.05$ Å^2, $B_{eq} \approx 4$ Å^2). Considering the isotropic thermal factor and the bond valence sum calculations developed by Altermatt and Brown [8] the oxygen atoms could be placed in either of the two 8h site. The valence v_{ij} of a bond between two atoms i and j is defined so that the sum of all the valence from a given atom i with valence V_i obeys:

$$\sum_j v_{ij} = V_i \quad \text{with } v_{ij} = \exp[(R_{ij} - d_{ij})/b].$$

d_{ij} is the length of the bond and b as 'universal' constant is equal to 0.37.

In the case of Ce1 in $Ce_3OF_3S_2$, the calculated values of V_i is 2.99 and this result is in good agreement with the theoretical value of 3. However the distance of 2.33 Å between Ce2 and O/F in the second 8h site leads to consider that this site is mainly occupied by oxygen. This short distance is indeed comparable to the Ce–O bond length in CeO_2 [9] and Ce_2O_2S [10]. The bond distances are reported in Table 2. In order to confirm this structural hypothesis, a Rietveld analysis has been performed on the powder X-ray diffraction pattern of $La_3OF_3S_2$ compound. The refinement factors are rather high due to the presence of very small amount of $La_2O_{1.5}FS$ phase which has not been taken into account in this refinement. However the results confirm that $La_3OF_3S_2$ and $Ce_3OF_3S_2$ are isostructural (Table 1).

The structure of $Ce_3OF_3S_2$ is presented in Fig. 1. This structure derives from LnSF and $Ln_2AF_4S_2$ networks. $[Ce_3OF_3]^{4+}$ sheets alternate with double layers of sulfur atoms with $[S_2]^{4-}$ formula. In $Ce_3OF_3S_2$ the Ce1 (4g site) is 6-fold coordinated to fluorine and 2-fold coordinated to oxygen, whereas Ce2 (8h site) is 3-fold coordinated to fluorine and only one to oxygen and finally 5-fold coordinated to sulfur atoms. The coordination polyhedron of rare earth has been defined by choosing appropriate F/O anions in accordance with bond lengths calculations. An alternative description could consider that as the Ce(2) atoms are roughly in the same plane as the sulfur atoms. Thus the structure could also be summarized as the stacking along c-axis of $[Ce(1)OF_3]$ and $[Ce(2)_2S_2]$ layers. These blocks derive re-

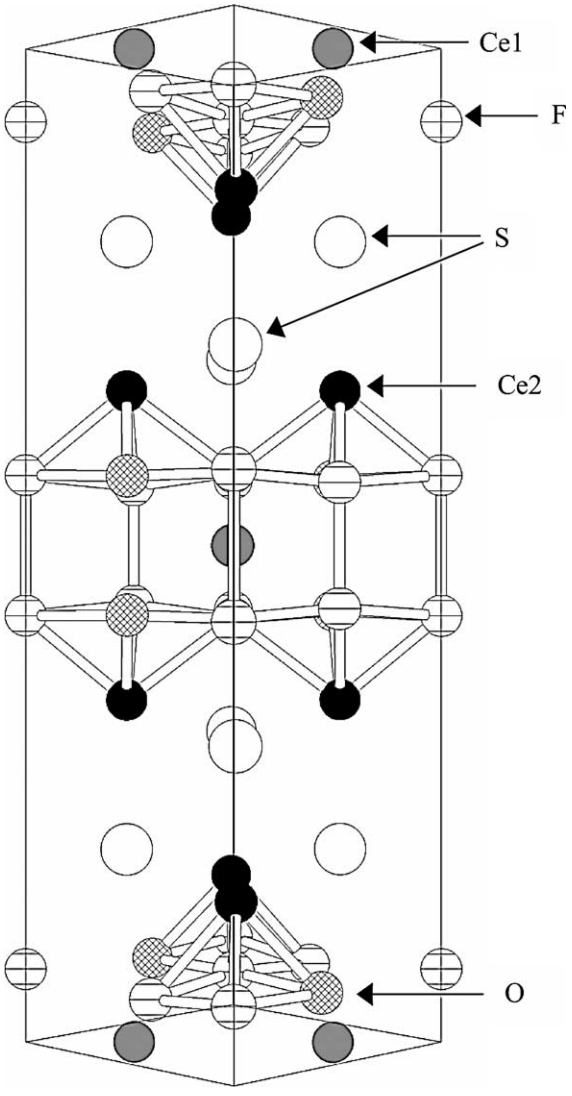

Fig. 1. Crystal structure of $Ce_3OF_3S_2$.

spectively from fluorite type, with edge shared cubes for [Ce(1)OF_3] and rock-salt structure for [$Ce(2)_2S_2$]. In the following we have chosen the former representation because it better takes into account the complete coordination of Ce2 (O/F/S), which appears to be responsible of the absorption properties (see below).

3.1.2. $La_2O_{1.5}FS$

The ratio O/F has been confirmed by a chemical analysis. This structure is close to that of $Ce_2O_{2.5}S$, the oxidized form of Ce_2O_2S, determined by Mauricot et al. [11]. The neutron and X-ray powder diffraction patterns of $La_2O_{1.5}FS$ could easily be indexed in the same $P\text{-}3m1$ space group. First a Rietveld refinement based on the atomic positions of La_2O_2S led to a good agreement between the calculated and observed X-ray diffractograms but to a large discrepancy between their neutrons counterparts. As previously proposed by Mauricot et al. [11] for $Ce_2O_{2.5}S$ composition, the insertion of an anion (oxygen or fluorine) in the half occupied 1b (0, 0, ½) position, greatly improved this refinement. However, the isotropic displacement parameter of this atom inflated to the very large value of 15 Å^2 (B_{eq}). The choice of 6i ($x, -x, z$) position, with an occupancy factor equal to 0.0833, gave satisfactory results with an improvement of the isotropic displacement parameter from 15 Å^2 (B_{eq}) down to 3 Å^2 (B_{eq}). The final reliability factors are $R_p = 2.05\%$, $R_{wp} = 2.76\%$ for the neutron diffractogram (see Fig. 2) and $R_p = 10.42\%$, $R_{wp} = 6.05\%$ for the X-ray counterpart. The O/F ratio of the anions present in the two sites 2d (1/3, 2/3, z) and 6i (x, $-x$, z) cannot be determined from the refinements even by taking into account valence band calculations, as used in the case of $Ce_3OF_3S_2$ composition. The results of the refinements are collected in Table 1. The bond distances are reported in Table 3.

Table 3
Interatomic distances in $La_2O_{1.5}FS$

$La_2O_{1.5}FS$ interatomic distances			
La–S	3.063(6) × 3	F/O1–F/O1	3.013(2) × 3
La–F/O1	2.445(2) × 3	F/O1–F/O2	2.61 average
	2.459(7) × 1		
		S–F/O1	3.468(6) × 6
La–F/O2	2.475(2) shortest	S–F/O2	3.495 average

The structure of $La_2O_{1.5}FS$ is similar to that of Ln_2O_2S, where Ln_2O_2 layers alternate with sulfur planes. An important feature of this structure is the presence of a hexagonal prismatic bipyramidal cavity, shown in Fig. 3. In $La_2O_{1.5}FS$, the extra anion (fluorine or oxygen) does not occupy the center of the cavity, but is off-centered as shown in Fig. 3. In addition all the cavities are not occupied by the extra anion, since the cavity occupation probability is only equal to ½. Thus lanthanum ions are surrounded by three sulfur atoms, four F/O anions and additional fluorine/oxygen corresponding to extra anions. The number of extra fluorine/oxygen may vary from 0 to 3. Thus the coordination number of La varies from 7 to 10.

3.2. Structural features of rare earth fluorosulfides and oxyfluorosulfides

As the anion polarizabilities differ, the resulting structures often show strong anisotropy with layer structures. This is the case of fluorohalides, such as EuFCl [12] of the PbFCl type, $Ba_{12}Cl_5F_{19}$ or $Ba_7Cl_2F_{12}$, with networks related to BaF_2 fluorite-type structure [13]. The five mixed anions structures α-LnSF, $Ln_2CaF_4S_2$, $Ln_3OF_3S_2$, $Ln_2O_{1.5}FS$ and Ln_2O_2S can be described as an intergrowth of layers. The first three correspond to the PbFCl type, whereas the two other ones are related to the La_2O_3-type structure. The structural parameters as well as bond distances of these phases are summarized in Table 4.

3.2.1. Structures related to PbFCl type

This structure can be considered as a stacking of $[Pb_2F_2]^{2+}$ sheets and double $[Cl_2]^{2-}$ chlorine atoms layers.

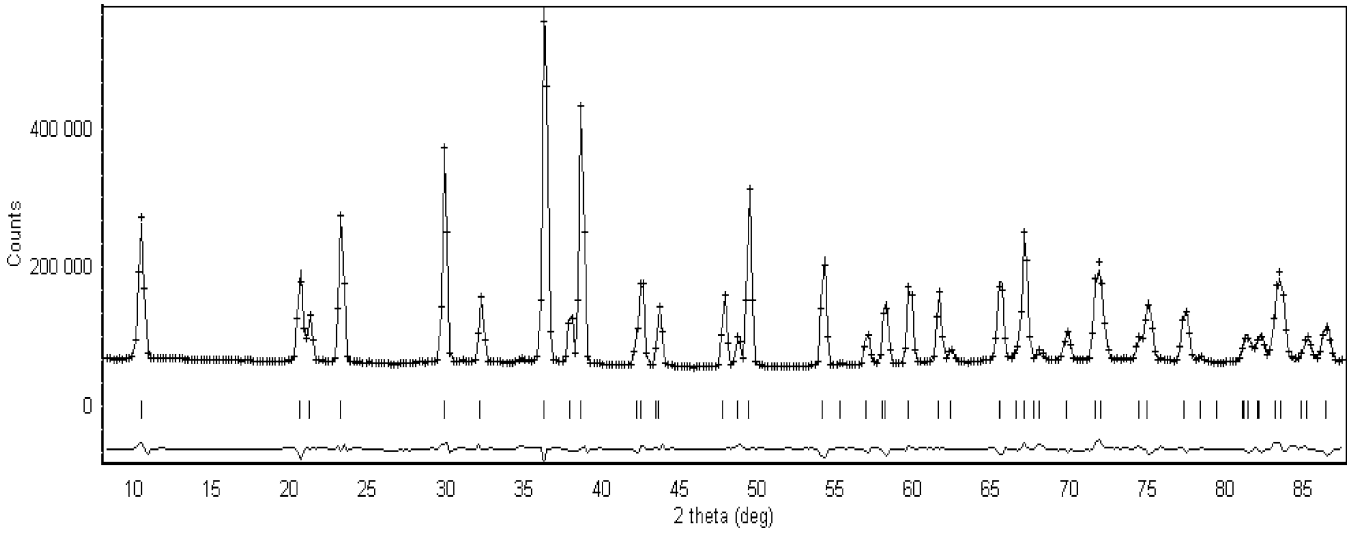

Fig. 2. Observed (+), calculated (full line) neutrons patterns and difference curve of $La_2O_{1\,5}FS$.

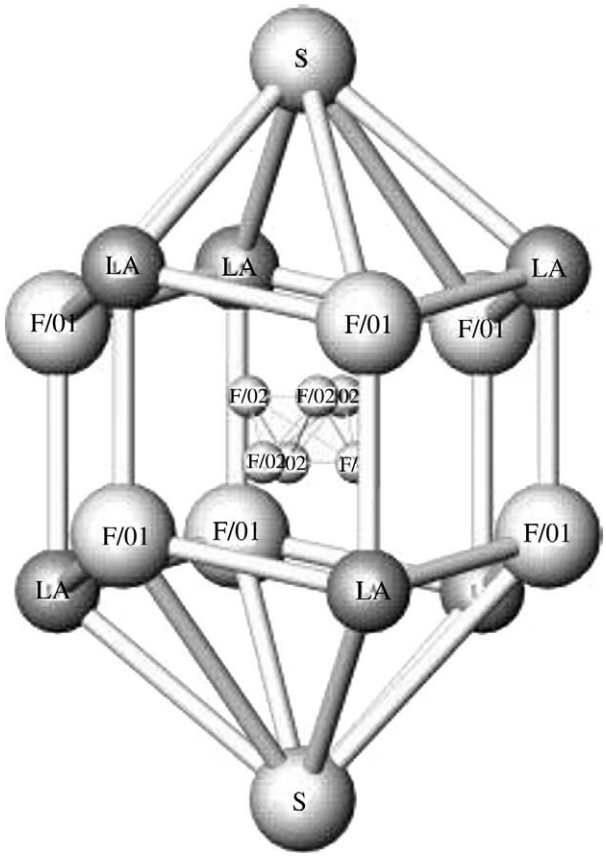

Fig. 3. Statistical occupation of F/O2 atoms in the hexagonal prismatic bipyramidal cavity of $La_2O_{1\,5}FS$.

Table 4
Unit-cell constants, space group and bond distances for some lanthanum oxysulfides, fluorosulfides and oxyfluorosulfides

Compounds	S.G. Cell parameters (Å)	d(La–X) (Å)
La_2O_2S [7]	P-3m1 $a = 4.05$, $c = 6.94$	d(La–O) = 2.423 × 3 d(La–O) = 2.424 × 1 d(La–S) = 3.037 × 3
$La_2O_{1\,5}FS$	P-3m1 $a = 4.111$, $c = 6.917$	d(La–F/O1) = 2.445 × 3 d(La–F/O1) = 2.459 × 1 d(La–S) = 3.064 × 3 d(La–F/O2) = 2.475 shortest
$La_3OF_3S_2$	$Pnnm$ $a = 5.804$, $b = 5.784$ $c = 19.482$	1st site d(La–F1) = 2.57 × 1 d(La–F2) = 2.44 × 1 d(La–F3) = 2.59 × 1 d(La–O) = 2.35 × 1 d(La–S) = 2.88 × 1 d(La–S) = 2.99–3.01 × 4 2nd site d(La–F1) = 2.44 × 2 d(La–F2) = 2.39 × 2 d(La–F3) = 2.59 × 2 d(La–O) = 2.46 × 2
$La_2CaF_4S_2$ [6]	$I4/mmm$ $a = 4.01$, $c = 19.45$	1st site d(La–F) = 2.40 × 4 d(La–S) = 2.94 × 4 d(La–S) = 3.02 × 1 2nd site d(La–F) = 2.41 × 8
LaSF [6]	$P4/nmm$ $a = 4.04$, $c = 6.97$	d(La–F) = 2.58 × 4 d(La–S) = 2.98 × 4 d(La–S) = 2.91 × 1

In α-LnSF the rare earth and fluorine atoms form $[Ln_2F_2]^{4+}$ layers where Ln_4F tetrahedral share four edges with four neighboring in a tetragonal arrangement. In order to balance the charges, the $[Ln_2F_2]^{4+}$ layers alternate with double $[S_2]^{4-}$ layers along the c-axis. The crystal structure of α-LnSF is shown on Fig. 4. The rare earth is located at the center of a distorted square antiprism with four F atoms in one base and four S atoms in the other. A fifth Ln–S bond smaller than the other ones appears parallel to the c-axis (Fig. 5). Such a coordination is very typical of Sillen-phases [14]. In the structure of $Ln_2CaF_4S_2$ (Fig. 4), the $[Ln_2F_2]^{4+}$ lay-

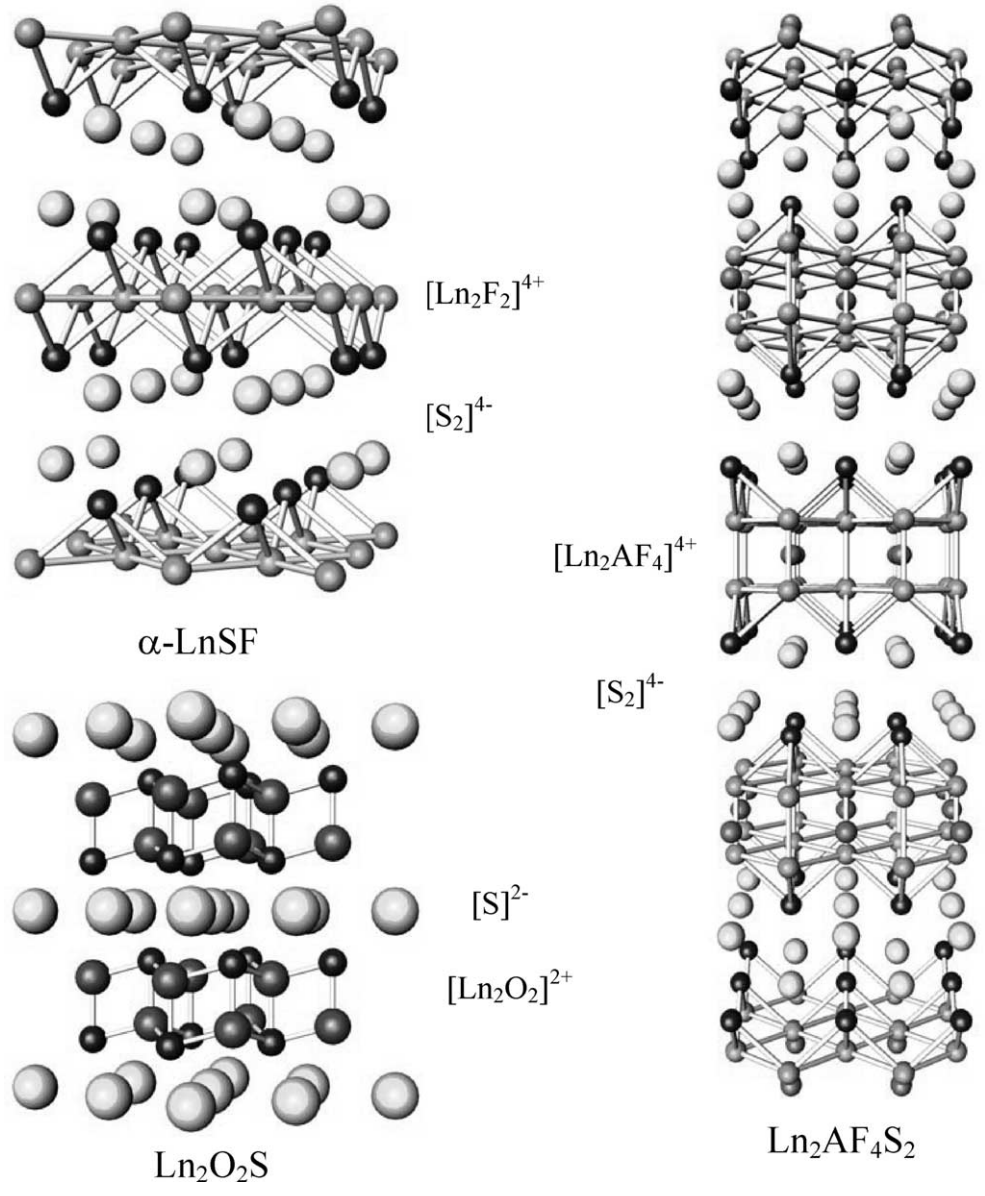

Fig. 4. Crystal structure of α-LnSF, Ln_2O_2S, and $Ln_2AF_4S_2$.

ers of LnSF are replaced by large and more complex sheets with $[Ln_2CaF_4]^{4+}$ formula. These sheets are always separated by double layers of sulfur atoms with $[S_2]^{4-}$ formula. In $Ln_2CaF_4S_2$, the rare earth occupies two sites which are also partially occupied by alkaline earth ions. It is relevant to notice that the lanthanide preferentially occupies the site surrounded by mixed anions (S, F) [6]. The Ln1 is 4-fold coordinated to fluorine and 5-fold coordinated to sulfur as in LnSF (Fig. 5), while Ln2 is 8-fold coordinated to fluorine. Moreover as far as the Ln–S bond distances are concerned, the fifth apical Ln–S bond length in LnSF (Ln = La–Nd), that is the shortest one: 2.91 Å, becomes the largest one in $Ln_2CaF_4S_2$ around 2.99 Å. This effect has been related to the reduction of the Ln–F bond lengths into the fluorite-type blocks [6]. The structure of the rare earth oxyfluorosulfides $Ln_3OF_3S_2$ corresponds to an orthorhombic distortion of the tetragonal cell of $Ln_2CaF_4S_2$ phase, with also two sites for the rare earth close to the Ln-sites of $Ln_2CaF_4S_2$. In $Ln_3OF_3S_2$ the increase of the Ln–F bond length in fluorite-type blocks with respect to that of $Ln_2CaF_4S_2$ composition contributes to the reduction of the Ln–S apical distance close to that of the LnSF phases. Moreover the occurrence of an orthorhombic cell for $Ln_3OF_3S_2$ phase, generates a dispersion of the Ln–F/O bond distances, whereas the Ln–S bond lengths do not vary too much and remain almost identical to those of LnSF compound.

3.2.2. Structures related to La_2O_3 type

Ln_2O_2S and $Ln_2O_{1.5}FS$ exhibit this type of structure. The Ln_2O_2S compounds (Ln = La to Yb and Y) have an hexagonal structure (S.G. P-3m1). Their atomic arrangement involves $[Ln_2O_2]^{2+}$ sheets and simple sulfur layers, as shown

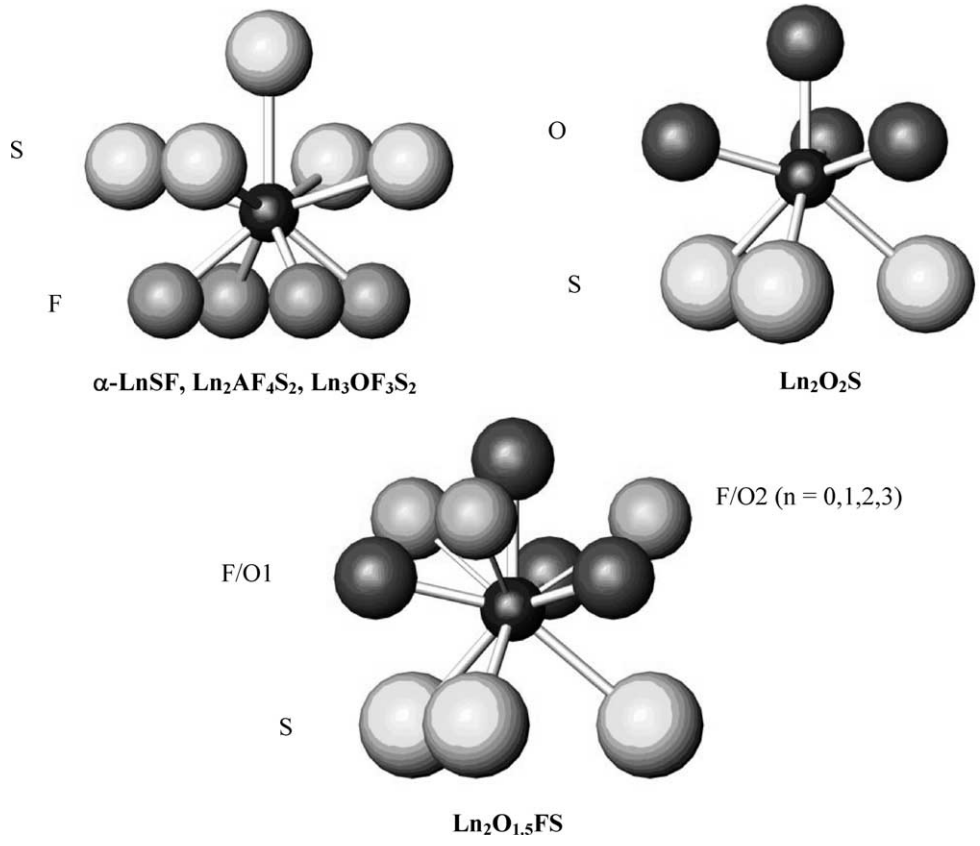

Fig. 5. Environnment of Ln in α-LnSF, $Ln_2AF_4S_2$, $Ln_3OF_3S_2$, Ln_2O_2S and $Ln_2O_{1.5}FS$ (the lanthanum site 8-fold coordinated to fluorine or oxygen atoms present in $Ln_2AF_4S_2$ and $Ln_3OF_3S_2$ structures has not been represented).

Table 5
Absorption edges (nm) determined from the diffuse reflectance curves of lanthanum oxysulfides, fluorosulfides and oxyfluorosulfides

Compounds	La_2O_2S	$La_2O_{1.5}FS$	$La_3OF_3S_2$	$La_2CaF_4S_2$	LaSF
Absorption edge (nm)	290 [16]	280	385	405	440

in Fig. 4. In this structure, the rare earth ion is located on a three-fold axis with a triangle of three sulfide ions on one side and a triangle of three oxide ions and one axial oxide ion on the other side (Fig. 5). $Ln_2O_{1.5}FS$ has the same structure with an extra anion number varying from 0 to 3 in the interstitial cavity (Fig. 3).

It is relevant to notice that the topology of [LnX] layers is different in the two structure types. Indeed in PbFCl-type structures [LnX] blocks derive from fluorite type structure with anions and cations located into separate planes perpendicular to the *c*-axis, whereas for La_2O_3-type structure cations and anions of [LnX] blocks are roughly in the same planes along the *c*-axis.

3.3. Optical properties

The diffuse reflectance spectra of various mixed anions rare earth compounds are represented in Fig. 6 ($La_3OF_3S_2$, LaSF, $La_2CaF_4S_2$, La_2O_2S and $La_2O_{1.5}FS$). The absorption edges corresponding to the maximum of the second derivative of the absorption curve are reported on Table 5. The

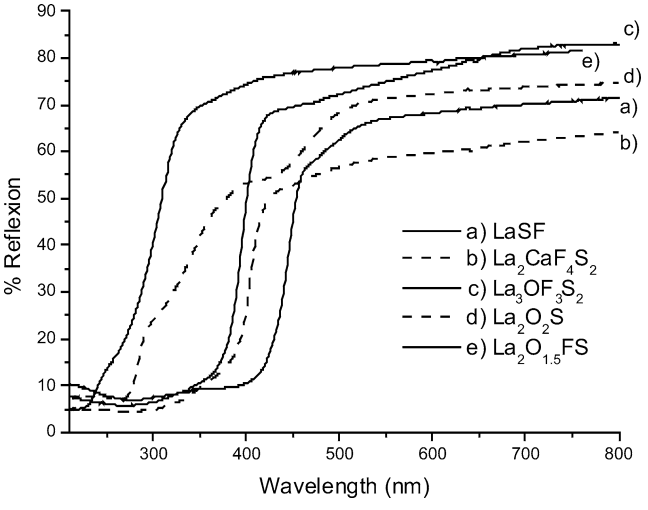

Fig. 6. Diffuse reflectance spectra of some lanthanum-based oxysulfides, fluorosulfides and oxyfluorosulfides.

spectrum of La_2O_2S exhibits a more complex structure characterized by three onset (290 nmn, 350 nm, 450 nm), the

two at higher wavelengths being usually attributed to absorption due to defect or exciton levels within the bandgap [15]. Therefore for La_2O_2S the selected value for the absorption edge, equal to 290 nm, corresponds to that the value measured by Borodulenko et al. [16].

4. Discussion

Because of the absence of f electrons, the absorption properties of lanthanum fluorosulfides, oxyfluorosulfides and oxysulfides are due to an electronic transfer between the valence band and the conduction band. The conduction band is characterized by the 5d states of the rare earth and the splitting of the 5d band is governed by the crystal field. The valence band is characterized by the 3p states of sulfur: the bandwidth increases as the La–S bond length decreases. The size or charge modulation of the sheet in the rare earth-based mixed anions compounds leads to a modification of the sulfur layers arrangement. Thus is it possible to modify the characteristics of the bond lengths and consequently the UV-visible absorption properties. In this way the structural features of our lanthanum compounds have been correlated to the optical absorption. The second lanthanum site in which La cations are 8-fold coordinated to fluorine or oxygen atoms in $La_2AF_4S_2$ and $La_3OF_3S_2$ phases (see Table 5) should not be considered in the near UV-visible absorption process because as in LaOF or LaF_3 compounds [17], the absorption edge should appear below 250 nm.

Thus a relevant parameter seems to be the number of sulfur atoms coordinated to the rare earth ions. In La_2O_2S, La is 3-fold coordinated to sulfur and in PbFCl-type compounds La is 5-fold coordinated to sulfur whereas the number of smaller anions (F, O) remains almost identical. The absorption edges of the La_2O_3-type phases are around 300 nm and for the other compounds (PbFCl type), around 400 nm. This is probably due to increasing nephelauxetic effect with increasing sulfur content in the coordination sphere of the rare earth. Usually both nephelauxetic effect and crystal field splitting decrease as the coordination of the central atom, surrounded by identical anions or anions having the same polarizabilities, increases. In our case, whereas the number of the smaller anions (O, F) remains almost identical, the number of sulfur atoms, the most polarisable species, varies from 3 (La_2O_2S, $La_2O_{1.5}FS$) to 5 (LaSF, $La_2CaF_4S_2$, $La_3OF_3S_2$). The absorption edge increases with the number of sulfur atoms around the rare earth. Since the five Ln–S bond lengths in LnSF-related structures are always smaller than the three ones in La_2O_2S related structures, one should point out surprisingly in the present case that the $[La(F,O)_4S_5]$ polyhedra are more covalent than the $[La(O,F)_4S_3]$ polyhedra in La_2O_2S related structures

For the compounds with double sulfur layers, LaSF, $La_2CaF_4S_2$ and $La_3OF_3S_2$, the absorption takes place in the 380–440 nm range. In $La_2CaF_4S_2$ the La–F bond lengths in the 9-fold coordinated site are strongly shorter than in LaSF. Moreover in the former compound the local La–S neighborhood corresponds to four short Ln–S bonds and one longer apical Ln–S bond. This effect is due to the presence of calcium in the structure. The Ca–F bond has a strong ionic character ($\chi_{Ca} = 1$ and $\chi_F = 4$, Pauling scale). Thus the competitive La–F bond ($\chi_{La} = 1.1$, Pauling scale) becomes more covalent and shorter. The $[La_2CaF_4]^{4+}$ block is also more compact than the $[La_2F_2]^{4+}$ block. The ionicity of the La–F bond decreases in $La_2CaF_4S_2$, compared to LaSF. As a consequence the nephelauxetic effect associated to sulfur anions decreases as well as the overlap of 3p (S) orbitals. The value of the bandgap increases and the absorption edge shifts to the UV range. The structure of $La_3OF_3S_2$ is similar to $La_2CaF_4S_2$. The calcium atom is substituted by lanthanum and one oxygen atom substitutes one fluorine atom. The presence of oxygen atoms in a compact block leads to the occurrence of shorter La–O distance and consequently larger competitive La–F bond length close to LaSF ones. The increase of the covalency in fluorite-type blocks due to the presence of oxygen atom leads to relax the La–S bonds and to decrease the nephelauxetic effect associated to the sulfur atoms. Thus the absorption edge related to the optical bandgap appears around 385 nm. It is relevant to mention again that UV-visible absorption spectra can be easily

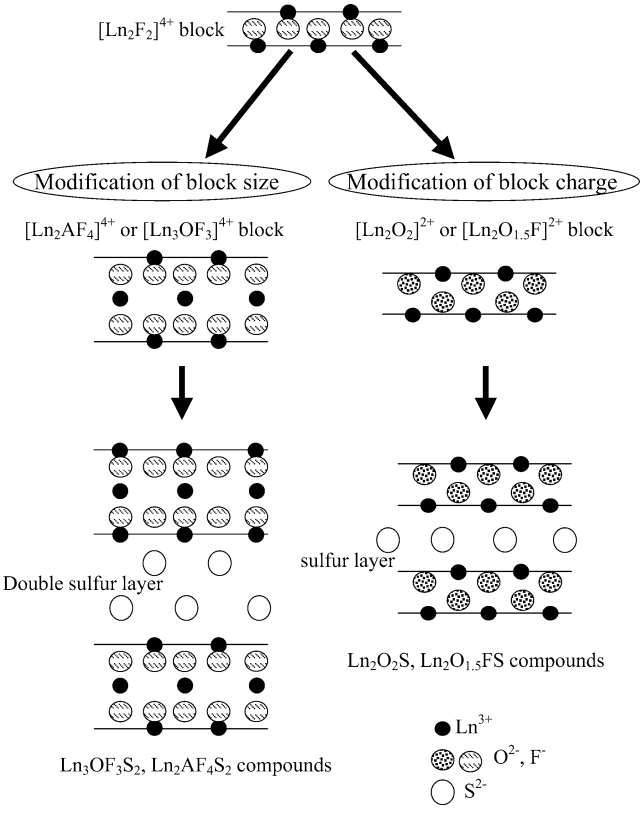

Fig. 7. Principle of building for the rare earth (oxy)fluorosulfides and oxysulfides networks.

interpreted, because both size particles and distribution are comparable.

The absorption edge of $LaO_{1.5}FS$ compound appears at 280 nm. This evolution is likely due to the reduction of oxygen content in rare earth sheets compared to La_2O_2S composition and to the increase of the rare earth coordination number. Thus the nephelauxtic effect as well as the crystal field splitting decrease and the value of the bandgap slightly increases.

The building of the mixed anions compounds networks plays a key role in the optical properties of these materials. The modulation of the rare earth fluorosulfides, oxyfluorosulfides and oxysulfides compositions is now wide open and the variable parameters are: the charge, size, geometry and composition of the rare earth blocks as well as the number and arrangement of the sulfur layers. The building principle of rare earth (oxy)fluorosulfides and oxysulfides networks is represented on Fig. 7.

5. Conclusions

Two new series of rare earth oxyfluorosulfides $Ln_2O_{1.5}FS$ and $Ln_3OF_3S_2$ have been prepared by solid state route. The crystal structures have been determined on the basis of XRD and neutron diffraction data (powder and single crystals). These compounds exhibit a bidimensional structure as rare earth oxysulfides and fluorosulfides. Single or double sulfur layers alternate with $[Ln_2O_{1.5}F]^{2+}$ and $[Ln_3OF_3]^{4+}$ rare earth oxyfluoride blocks.

The diffuse reflectance spectra of the five compositions La_2O_2S, $La_2O_{1.5}FS$, LaSF, $La_2CaF_4S_2$ and $La_3OF_3S_2$ have been measured. Structural features have been correlated to optical absorption properties. The electronic transitions at the origin of the absorption for these compounds result from charge transfer mechanism from 3p (S) band to 5d (La) ones. The characteristics of the rare earth sheets (bondlength, composition) and the number of sulfur atoms around the rare earth have been linked to the nephelauxetic effect and the crystal field splitting. Theses parameters explain the variation of the absorption edge according to the rare earth mixed anions composition.

Acknowledgement

This work has been supported by Rhodia Chimie (Centre de Recherche d'Aubervilliers-France).

References

[1] L. Ozawa, H. Forest, Anal. Chem. 45 (1973) 978.
[2] G. Blasse, B.C. Grabmaier, Luminescent Materials, Springer-Verlag, Berlin, Heidelberg, 1994, p. 161.
[3] A. Demourgues, A. Tressaud, H. Laronze, P. Macaudière, J. Alloys Comp. 323–324 (2001) 223.
[4] V. Petricek, M. Dusek, The crystallographic computing system JANA2000, Institute of Physics, Praha, Czech Republic, 2000.
[5] B.A. Hunter, RIETICA Rietveld analysis using a Visual Interface, Australian Nuclear Science and Technology Organisation, Menai, N.S.W., Australia, 2001.
[6] A. Demourgues, A. Tressaud, H. Laronze, P. Gravereau, P. Macaudière, J. Fluor. Chem. 107 (2001) 215.
[7] B. Morosin, D.J. Newman, Acta Cryst. B 29 (1973) 2647.
[8] D. Altermatt, I.D. Brown, Acta Cryst. A 43 (1987) 125.
[9] E.A. Kuemmerle, G. Heger, J. Solid State Chem. 147 (1999) 485.
[10] W.H. Zachariasen, Acta Cryst. 2 (1949) 60.
[11] R. Mauricot, J. Gareh, M. Evain, Z. Kristallogr. 212 (1997) 24.
[12] B. Tanguy, M. Pezat, A. Wold, P. Hagenmuller, C.R. Acad. Sci. 280 (1975) 1347.
[13] A. Es-Sakhi, A. Garcia, L. Struye, P. Willems, P. Leblans, A. Moudden, C. Fouassier, Mater. Sci. Eng. B, in press.
[14] J.F. Ackerman, J. Solid State Chem. 62 (1986) 92.
[15] O. Schevciw, W.B. White, Mat. Res. Bull. 18 (1983) 1059.
[16] G.P. Borodulenko, Y. Bykovskii, A. Kirillovich, M. Ponomarev, Z. Pukhlii, Soviet Physics Solid State 29 (1987) 507.
[17] V.A. Lobach, B.V. Shul'gin, I.N. Shabanova, V.A. Trapeznikov, N.P. Sergushin, A.A. Sabol', Soviet Physics Solid State 20 (1978) 1155.